Muc5ac null mice are predisposed to spontaneous gastric antro-pyloric hyperplasia and adenomas coupled with attenuated *H. pylori* induced corpus mucous metaplasia

Sureshkumar Muthupalani[1], **Zhongming Ge**[1], **Joanna Joy**[1], **Yan Feng**[1], **Carrie Dobey**[1], **Hye-Youn Cho**[2], **Robert Langenbach**[3], **Timothy C Wang**[4], **Susan J Hagen**[5], **James G Fox**[*,1,6]

[1]Division of Comparative Medicine, Massachusetts Institute of Technology, Cambridge, MA 02139

[2]Immunity, Inflammation and Disease Laboratory, National Institute of Environmental Health Sciences, National Institutes of Health, Research Triangle Park, NC 27709

[3]Laboratory of Toxicology and Pharmacology, National Institutes of Health, National Institute of Environmental Health Sciences, Research Triangle Park, NC 27709

[4]Division of Digestive and Liver Diseases and Herbert Irving Cancer Research Center, Columbia University College of Physicians and Surgeons, New York, NY 10032

[5]Department of Surgery/Division of General Surgery, Beth Israel Deaconess Medical Center, Boston, Massachusetts; Harvard Medical School, Boston, MA.

[6]Department of Biological Engineering, Massachusetts Institute of Technology, Cambridge, MA 02139

Abstract

Gastric cancer (GC) is the third leading cause of cancer-related deaths worldwide and is strongly associated with chronic *Helicobacter pylori* (*Hp*) infection. The ability of *Hp* to closely adhere to the gastric surface protective mucous layer containing mucins (MUC in humans and Muc in animals), primarily Muc5ac, is integral in the step wise pathogenesis from gastritis to cancer. To probe the role of Muc5ac in *Hp*-induced gastric pathology, *Muc5ac*^{−/−} and *Muc5ac*^{+/+} (WT) mice were experimentally infected with *Hp* Sydney strain (SS1). At 16 weeks and 32 weeks post infection (wpi), groups of mice were euthanized and evaluated for the following: gastric histopathological parameters, immunohistochemical expression of mucins (Muc5ac, Muc1, Muc2), Trefoil factor family proteins (Tff1 and Tff2), *Griffonia (Bandeiraea) simplicifolia* lectin II (GSL II) (mucous metaplasia marker) and Clusterin (Spasmolytic Polypeptide Expressing Metaplasia (SPEM) marker), *Hp* colonization density by qPCR and gastric cytokine mRNA levels. Our results demonstrate that *Muc5ac*^{−/−} mice developed spontaneous antro-pyloric proliferation, adenomas and in one case with neuroendocrine differentiation; these findings were independent of *Hp* infection along with strong expression levels of Tff1, Tff2 and Muc1. *Hp*-infected *Muc5ac*^{−/−}

[*]**Corresponding Author:** James G. Fox, 77 Massachusetts Avenue, 16-825C, Cambridge, MA 02139, Jgfox@mit.edu.

mice had significantly lowered gastric corpus mucous metaplasia at 16wpi and 32 wpi (P=0.0057 and P=0.0016, respectively), with a slight reduction in overall gastric corpus pathology. GSII positive mucous neck cells were decreased in *Hp*-infected *Muc5ac$^{-/-}$* mice compared to WT mice and clusterin positivity was noted within metaplastic glands in both genotypes following *Hp* infection. Additionally, Hp colonization densities were significantly higher in *Muc5ac$^{-/-}$* mice compared to WT at 16 wpi in both sexes (P=0.05) along with a significant reduction in gastric *Tnfα* (16 wpi- males and females, P=0.017 and P=0.036, respectively and 32 wpi- males only, P=0.025) and *Il-17a* (16 wpi- males) (P=0.025). Taken together, our findings suggest a protective role for MUC5AC/Muc5ac in maintaining gastric antral equilibrium and inhibiting *Hp* colonization and associated inflammatory pathology.

Keywords

MUC5AC/Muc5ac; Mucins; *H. pylori*; Metaplasia; Pyloric adenoma

INTRODUCTION

A central paradigm in the chronic inflammation driven pathogenesis of *Helicobacter pylori* associated gastric cancer is the organism's inherent ability to establish successful colonization niches in the gastric mucus and also it's ability to adhere to the gastric epithelium (1). A complex interplay exists between *Hp* and the host's gastric mucosa leading to persistent *Hp* colonization within the stomach often for a lifetime (1, 2). The gastric lumen-surface epithelial interface is characterized by its' acidic pH, lack of nutrients, high viscosity mucus, continuous clearance of luminal contents by peristaltic action, epithelial cell turnover, infiltrating inflammatory cells and the host's innate and adaptive immune responses (3, 4, 5). Upon gastric infection, *Hp* encounters the protective mucous layer which is composed primarily of mucins and many other glycoproteins (3, 4, 5). Mucins are high molecular mass, heavily glycosylated, oligomeric substances secreted on the cell surface associated with glycoproteins present within the mucous and the surface epithelium; nearly 21 different mucin forms have been identified in humans and to a large extent in mice (4–6). The secreted mucins, MUC5AC and MUC6, and the cell surface mucin, MUC1, form the major gastric mucins in the human stomachs (4, 5), and have similar expression profiles in mice (7). However, in the diseased stomach secondary to *Hp*-induced mucosal alterations, de-novo expression of intestinal mucins namely MUC2, MUC4, MUC5B and MUC13 has been documented in humans and animal models (8–12). MUC5AC/Muc5ac is the major mucin in the stomach secreted by mucous cells on the surface foveolar epithelium of humans and mice and is localized along the adherent mucous layer (7). Muc6 is primarily expressed within deeper glands and mucous neck cells, whereas Muc1 is primarily distributed along the foveolar cell surface epithelium mimicking the Muc5ac expression pattern and is also expressed minimally within mucous neck cells (10, 12, 13).

In mice and Mongolian gerbils, *H. pylori* mostly resides within 25μM of the mucosal surface with high densities of motile organisms in the juxta-mucosal region (10μM distance) where the pH gradient is less acidic than the luminal space (14). This site predilection is reflective of the close interaction between *Hp* adhesins with host mucins and other cell surface

receptors (15). Blood group fucosylated antigens such as Lewis a and b (Le^a and Le^b) and H- type antigens are known to be highly expressed in epithelial cell surfaces and associated with gastric mucins, chiefly MUC5AC (16). Interestingly, Le^b is the major receptor for one of the best characterized adhesins of *Hp*, namely the blood group binding antigen, BabA (1, 2 3, 15–17). As MUC5AC/Muc5ac is a major binding factor for *H. pylori* in the stomach (3, 17, 18), we sought to further investigate the role of Muc5ac in *H. pylori* pathogenesis in a mouse model deficient in Muc5ac. Briefly, the study was conducted using a well characterized chronic *Hp* SS1 infection model in *Muc5ac*$^{-/-}$ and WT mice to compare the differences in gastric pathology scores, colonization densities and gastric cytokine responses at two post infection time points, specifically at 16 and 32 weeks post infection (wpi).

METHODS

Experimental mice and bacterial infection protocol

Muc5ac$^{-/-}$ mice were obtained from the National Institute of Environmental Sciences (NIEHS) where they had been developed by deleting exons 21–31 the exons coding for the major glycosylation sites in Muc5ac and maintained on a C57/BL6–129 Ola background for 15 generations. The genotype of these animals was confirmed using PCR, Northern blot and stomach Muc5ac immunohistochemistry analyses prior to shipping these mice to MIT. AT MIT, the mice were re-derived by embryo transfer prior to experimental usage. Five-week-old male and female C57BL/6–129 0la mice (referred to as wild type mice –WT) were obtained from Taconic Farms (Germantown, NY). The WT mice as well as *Muc5ac*$^{-/-}$ mice, were housed under specific-pathogen-free (SPF) conditions (free of *Helicobacter* spp., *Citrobacter rodentium*, *Salmonella* spp., endoparasites, ectoparasites, and exogenous murine viral pathogens) in an AAALAC accredited facility. All animal housing conditions and experimental protocols were approved by the MIT Committee on Animal Care. The various groups of mice (Table 1) at 7 weeks of age were orally gavaged with either *Hp* strain SS1 (*Hp* SS1) as described earlier (19, 20) every other day for 6 days with 3 doses of 0.2 ml (~2 × 10^8 organisms) or 3 sham doses of 0.2ml sterile Brucella broth.

Gross necropsy and tissue collection protocols

After dosing, the mice were euthanized at 16wpi and 32wpi by CO$_2$ euthanasia followed by gross necropsy and tissue collection procedures as previously described with slight modifications (21, 22). Briefly, the stomach was opened along the lesser curvature and evaluated for any gross abnormalities. Representative longitudinal sections of the stomach extending from the squamous forestomach to the pyloric duodenum were collected and fixed in 10% neutral buffered formalin. These fixed sections were then processed by standard paraffin embedding, 5μM sectioning and hematoxylin and eosin (H&E) staining protocols. Representative sections of the stomach corpus and antrum were also collected for RNA/DNA extraction as described below. Additionally, archival stomach sections from the original WT and *Muc5ac*$^{-/-}$ male mice at 10–12months of age were obtained from NIEHS. The corpus and antrum from these mice were also evaluated to compare the gastric phenotypes of WT and *Muc5ac*$^{-/-}$ mice housed under different environmental conditions.

Histopathological Evaluation

H&E slides of the stomach were graded by a comparative pathologist (S. M) blinded to sample identity separately for both the corpus and antrum/pylorus. In the corpus, the categories scored were inflammation, epithelial defects, atrophy, hyperplasia, pseudopyloric metaplasia, dysplasia, and mucous metaplasia on an ascending scale from 0 to 4 based on severity using criteria previously described with slight modifications (21, 22). Gastric histological activity indices (GHAI) were generated by computing the sum of all individual sub-categorical scores except hyalinosis which can be a spontaneous non-specific alteration in murine stomach. Adapting the same grading scheme the antrum/pylorus was also scored for inflammation, epithelial defects, hyperplasia and dysplasia with the sum of all these categories represented as total antral pathology scores (21, 22). Briefly, inflammation was evaluated on the basis of amount and extent of leukocyte infiltration in the mucosa and submucosa of the stomach. Epithelial defects were scored on the basis of the extent of surface epithelial degeneration, tethering, erosions to full thickness ulcerations. Hyalinosis is a non- specific change characterized by the accumulation of brightly eosinophilic droplets and/or extracellular crystals was scored the extent of gastric mucosal involvement (21, 22). Oxyntic atrophy was defined as a reduction in the mass of chief and parietal cells in the gastric corpus and graded on the extent of loss via cell loss and/or metaplastic transformation. Epithelial hyperplasia refers to expansion of the gastric mucosal thickness by proliferation of surface foveolar-type epithelium and/or antral-type glandular units and appropriately graded in relation to the extent of oxyntic loss (21, 22). Mucous metaplasia is usually associated with parietal and chief cell loss leading to expansion of gastric mucous neck cells (PAS+/Alcian blue/TFF2 + foamy cells with marginated nucleus resembling Brunner's glands) secreting a mixture of neutral and acidic mucins in the gastric corpus mucosa (21, 22). Pseudopyloric metaplasia is a preneoplastic change defined as replacement of the oxyntic mucosa by glands resembling antral phenotype with cells being more columnar and lacking typical cytoplasmic granules of oxyntic cells as well as the absence of cytoplasmic mucous appearance of mucous metaplasia. Spasmolytic Polypeptide Expressing Metaplasia (SPEM) is considered to be a molecular equivalent term for pseudopyloric metaplasia due to expression of Trefoil factor 2 (Tff2) but is also seen in murine mucous metaplasia (21, 22).

Gastric epithelial dysplasia is histologically an unequivocal neoplastic change without evidence of stromal invasion occurring in sessile, flat, depressed or elevated/polypoid mucosal lesions and is defined by both architectural abnormalities (haphazard glandular arrangement, loss of vertical orientation, back-to-back gland associations, branching, infolding, and piling up of cells) and cytological atypia (cellular pleomorphism, anisocytosis, anisokaryosis, ill-defined cellular junctions, loss of nuclear polarity, pencil or cigar shaped nuclei, hyperchromatic nuclei, increased nuclear–cytoplasmic (N–C) ratio, visible mitosis, bizarre mitotic figures) (21, 22). The term gastric adenoma was restricted to well demarcated or circumscribed, polypoid or raised nodular lesions comprising of tubular and/or villous structures, lined by dysplastic epithelium. Dysplasia/neoplasia was graded on its extent and severity of changes as follows: score of 0 for normal or mild simple epithelial hyperplasia with no atypia; score of 1 for one or few epithelial hyperplastic foci with mild architectural atypia (equivalent to indefinite for dysplasia or reactive epithelium); a score of

2 for atypical hyperplasia comprising of coalescing proliferative epithelial lesions with glandular architectural abnormalities (equivalent to indefinite for dysplasia); a score of 2.5 for low grade dysplasia/intraepithelial neoplasia or low grade adenoma and all of these proliferative lesions were defined by severe glandular architectural abnormalities and borderline cytological atypia; a score of 3 is equivalent to high grade dysplasia/ intraepithelial neoplasia or a high grade adenoma characterized by severe architectural and cytological atypia; a score of 3.5 for intramucosal invasive neoplasia (intramucosal carcinoma) characterized by high grade dysplastic lesions with unequivocal invasion into the lamina propria or muscularis mucosa (dysplasia score of 3.5; and a score of 4 for submucosal invasive neoplasia (submucosal carcinoma) for true unequivocal invasion into the gastric submucosa or beyond. This 4 point scoring system was adapted to reflect the limitations of the mouse models (21, 22) and correlated to human gastric dysplasia diagnosis and grading schemes (23).

Immunohistochemistry

Six representative formalin fixed and paraffin embedded stomach histological sections (3 M, 3F) from all the groups at 32wpi were used to perform a panel of specific immunohistochemical stains using the following rabbit polyclonal or mouse monoclonal antibodies to either human (reactive with mouse) or mouse specific antigens: a. rabbit origin- MUC5AC and MUC2 (Santa Cruz Biotechnology, Dallas, TX, USA), TFF2 (in-house rabbit polyclonal TFF2 antibody referenced in 21), MUC1, Clusterin and TFF1 (Life Span BioSciences, Seattle, WA, USA), NSE (Neuron specific enolase) (Thermo-Fischer Scientific Inc., Waltham, MA, USA), Chromogranin A (Novus Biologicals, Littleton, CO, USA & AbCam, Cambridge, UK), Cytokeratin 20 (CK20) (AbCam, Cambridge, UK); b. mouse origin: S100 (BioCare Medical, Pacheco, CA, USA). Additionally, gastric mucous neck cells were identified using fluorescein isothiocyanate (FITC)- conjugated *Griffonia (Bandeiraea) simplicifolia* lectin II (GSL II) and slides were mounted with Vectashield plus DAPI (4,6-diamidino-2-phenylindole) (Vector Laboratories, Burlingame, CA, USA). For chromogranin A peptide blocking immunohistochemistry, to identify non-specific staining if any, the chromogranin primary antibodies were mixed with varying concentrations of the full length human (full length) chromogranin A peptide (ab138920) AbCam, Cambridge, UK) for 1hr at room temperature prior to following routine immunostaining protocols. For routine immunohistochemistry, unstained paraffin embedded and sectioned stomach slides were incubated at 60 °C for 30 minutes, followed by de-paraffinization and rehydration prior to staining with specific antibodies as described earlier with slight modification (21). The antigens were retrieved at a low or high pH, depending on the antibody, by incubation for 45 minutes at 95°C and the slides were stained sequentially using an automated stainer (Lab Vision Autostainer 360; Thermo Fisher Scientific, Waltham, MA, USA) incorporating a 10-min Ultravision peroxidase block, for a 30-min Rodent block R, and primary antibodies for 30 minutes. This was followed by appropriate species specific secondary polymer based antibodies, and subsequent development with diaminobenzidine (DAB), counterstained with hematoxylin. Slides were dehydrated and cleared, and then cover slipped for qualitative assessment of the expression pattern of the various markers.

Quantitation of *Hp* SS1

At necropsy, gastric contents were removed by rinsing with sterile PBS and one-cm segments of piece of gastric tissue containing the corpus and antrum for isolation of RNA or DNA were collected and frozen in liquid nitrogen immediately and stored at –70°C prior to use. DNA from the samples was extracted using the High Pure PCR Template Preparation Kit (Roche, Applied Science, and Indianapolis, IN). Colonization levels of *Hp* SS1 from the glandular portion of the stomach (antrum and corpus) were quantitatively measured using the primers and probe complementary to the *Hp ureB* gene qPCR in the 7500 FAST Real-time PCR System (Life Technologies) in as described previously (20). The copy numbers of the *Hp* genome as measured by qPCR were then normalized to µg of mouse chromosomal DNA using the 18S rRNA gene-based primers and probe mixture (Life Technologies) (19, 20).

Expression of select gastric genes

For relative mRNA quantitation of selected genes, total RNA the gastric tissue was prepared using Trizol reagent according to manufacturer's recommendations (Invitrogen, Carlsbad, CA). Five µg of total RNA from each sample was converted into cDNA using the High Capacity cDNA Archive kit (Life Technologies). Levels of *Ifnγ, Tnfa, Il-1β, Il-17A, Il-10, Il-22* and *Tff2* mRNA in the gastric tissues were examined by qPCR using commercial primers and probes (TaqMan Gene Expression Assays) in the 7500 FAST Real-time PCR System. Transcript levels were normalized to the endogenous control glyceraldehyde-3-phosphate dehydrogenase mRNA (*Gapdh*) (19, 20).

Statistical analysis

Semi-quantitative histopathological scores from the corpus and antrum for different sub-categories and cumulative GHAI scores were compared across groups by the Kruskal-Wallis one-way analysis of variance with Dunn's posttest and between groups by the Mann-Whitney U test using Prism software (GraphPad, San Diego, CA) and graphs were represented as the median with the range. Quantitative data values generated for colonization levels of *Helicobacter* species and cytokine mRNA levels in the tissues were analyzed using the two-tailed Student *t* test. *P* values of <0.05 were considered significant.

RESULTS

Muc5ac$^{-/-}$ mice are predisposed to spontaneous antro-pyloric epithelial proliferation that is independent of *Hp* infection

The gastric antrum/pylorus of the experimental mice were scored for inflammation, edema, epithelial hyperplasia, dysplasia, and a cumulative total antral pathology index score was generated for group and time-wise comparative analysis (Figure 1A–D). Interestingly, uninfected *Muc5ac*$^{-/-}$ mice at 32wpi (39 weeks of age) had significantly higher total antral pathology index (P=0.0008) and dysplasia scores (P=0.0019) compared to uninfected WT mice (Figure 1B, D). The histopathological changes in the antrum and pylorus of these *Muc5ac*$^{-/-}$ mice included mild to moderate inflammation, epithelial defects including erosions and dilated glands, epithelial hyperplasia and progressive dysplasia resulting in

various categorical lesions as enumerated in Table 2. These lesions included normal with no hyperplasia/dysplasia (1/12), simple epithelial hyperplasia with no dysplasia (2/12), indefinite for dysplasia (reactive epithelium and/or atypical hyperplasia) (7/12), low grade adenoma (1/12) or high grade adenoma (1/12) (Figure 2G, H) compared to lack of similar range of proliferative and dysplastic lesions in the uninfected WT mice (Figure 1E, F and Table 2). Within the large adenoma in the pyloric region of the $Muc5ac^{-/-}$ mouse, there were multiple characteristic micronodular areas of divergent morphological appearance resembling rosettes that were presumed to be foci of possible neuro-endocrine differentiation. (Figure 1G, H, arrows). The antro-pyloric inflammation and proliferative changes were also observed in uninfected $Muc5ac^{-/-}$ mice at 16 wpi, but at a lesser magnitude with no significant dysplastic changes indicative of an age related progression in hyperplasia and dysplasia (Figure 1A, C).

The various antral pathological alterations were also observed in the Hp-infected $Muc5ac^{-/-}$ mice at both time points but were of lesser degree, resulting in significantly lowered total pathology index scores at 32 wpi (P=0.0467) as compared to their uninfected counterparts but with comparable median dysplasia scores though high grade adenoma was noted only in the uninfected cohort (Figure 1B, D, Table 2). The WT mice (both infected and uninfected) did not show similar antro-pyloric proliferative and dysplastic changes as observed in uninfected $Muc5ac^{-/-}$ mice at 32 wpi time point (Figure 1, Table 2). At 16 wpi, Hp-infected WT mice also showed significantly (P=0.009) higher total antral pathology index compared to uninfected WT but it was primarily due to mild extension of $H. pylori$-induced corpus inflammation and epithelial defects into the antrum (Figure 1A). This was not significant at 32 wpi (Figure 1B).

Given the fact that spontaneous gastric antro-pyloric lesions were noted in 10 month-old $Muc5ac^{-/-}$ mice (males only), we sought to rule out any possible institution related environmental or microfloral effects in these mice by analyzing uninfected (Hp free) archival gastric tissues from mice maintained at NIEHS. We observed similar pathological alterations in the gastric antrum and pylorus of 11 month-old $Muc5ac^{-/-}$ mice (Figure S1). Compared to WT (n=9), $Muc5ac^{-/-}$ male mice (n=11) developed significantly higher cumulative antrum/pylorus total pathology scores (Figure S1A), with higher scores for inflammation, epithelial defects, hyperplasia and dysplasia (Figure S1B, Table 2) including low grade adenoma (1/11) and high grade adenoma (1/11) (shown in Figure S1, C&D). We did not attempt to further classify the nature of antro-pyloric hyperplasia and adenoma into sub-categories such as foveolar, pyloric gland and intestinal type using additional markers such as Muc5ac (for foveolar adenoma but not useful in $Muc5ac^{-/-}$ mice) or Muc6 (no reliable commercially available antibody that works on murine tissues) but nevertheless, on the basis of morphology and lack of Muc2 immunostaining, most of these proliferative epithelial lesions were considered to be of either foveolar or mixed foveolar and pyloric glandular phenotype. Overall, we identified an age-associated phenotype of gastric antro-pyloric hyperplasia and dysplasia/adenoma progression independent of environmental effects in association with loss of Muc5ac function in murine stomach.

Immunohistochemical expression profiles of mucins and trefoil factors in the gastric antrum/pylorus of WT and *Muc5ac*−/− mice

Given the importance of mucins and trefoil factors in gastric homeostasis and *Helicobacter pylori* pathogenesis (24–28), we assessed the immunohistochemical expression patterns of these proteins in relation to the spontaneous antro-pyloric lesions in *Muc5ac*−/− mice. Of note, similar proliferative lesions involving the antrum have been documented in *Hp*-infected *Tff2*−/− mice on a CF57BL background (21). In addition, mice deficient in *Tff1* have also been shown to develop spontaneous antro-pyloric adenomas and carcinomas (29). The gastric antrum/pylorus of uninfected *Muc5ac*−/− mice did not express Muc5ac as expected, but showed moderate to strong expression of Muc1, Tff2 and Tff1 within the hyperplastic and neoplastic glandular and surface epithelium (Figure 2). The increase in expression levels of these proteins was correlated with increased epithelial mass as a result of epithelial hyper-proliferation. It should be noted that the occasionally observed neuroendocrine-like distinct micro-nodular foci within one large adenoma in the pylorus did not stain with the markers, Muc1, Tff2, and Tff1, suggestive of altered differentiation within the tumor. Additional characterization of these presumptive neuroendocrine like foci by immunohistochemistry using markers specific for neuroendocrine tumors as in humans (30), showed that these foci exhibited mild to moderate positivity with Neuron-Specific Enolase (NSE) (Figure S2). With Chromogranin A immunostaining, these foci showed only non-specific background extracellular staining as demonstrated by a Chromogranin A blocking peptide incubation protocol in Figure S2. In addition, these neuroendocrine foci or rosettes and surrounding proliferative villo-tubular glands failed to react with the neuronal marker, S100 (not shown). Chromogranin A is typically present in most gastric neuroendocrine tumors (30) and its absence in our case was intriguing and may require additional testing but was not pursued due to tissue limitations and rarity of these neuroendocrine foci within gastric antro-pyloric proliferative lesions of *Muc5ac*−/− mice. However, cytokeratin 20 (CK20), an epithelial marker for intestinal epithelium/goblet cells as well for gastric foveolar epithelium, was not expressed within the antro-pyloric rosettes (NSE positive areas) of *Muc5ac*−/− stomach as shown in Figure S2. Other than Muc2, which is not typically expressed in the normal stomach, all other mucins and trefoil factors displayed their typical immunostaining pattern in the antrum/pylorus of the WT murine stomach (Figure 2), with the expression patterns of Muc5ac and Muc1 more or less similar in distribution. In addition, *Hp* infection did not alter the overall antro-pyloric expression patterns of mucins (Muc1, Muc5ac, Muc2) and trefoil factors (Tff1 and Tff2) in both WT or *Muc5ac*−/− mice (data not shown).

Hp infection led to attenuation of gastric corpus mucous metaplasia in *Muc5ac*−/− mice

Hp-infected WT and *Muc5ac*−/− mice at both 16 wpi and 32 wpi had significantly higher corpus GHAI scores than their uninfected counterparts (Figure 3A, C) (WT Hp vs WT uninfected, 16wpi, 32wpi: P=0.0005, P=0.0002/*Muc5ac*−/− Hp vs *Muc5ac*−/− uninfected, 16wpi, 32wpi: P=0.0013, P=0.029), .Representative images of the gastric corpus from various groups are depicted in Figure 3E–H. However, there was no significant difference in corpus GHAI between the two infected groups at both time points, though Hp infected *Muc5ac*−/− mice at both time points showed a trend towards lesser overall corpus pathology. Within each infected group there was also no appreciable gender differences on the severity of gastric corpus pathology. Gastric corpus mucous metaplasia was also significantly (P=

0.0012–0.0021) increased by *Hp* infection in WT mice as compared to their uninfected counterparts at both 16 wpi and 32 wpi (Figure 3B, D). However, in the Hp infected *Muc5ac*$^{-/-}$ mice, mucous metaplasia was significantly increased during Hp infection only at 16wpi (Figure 3B, P= 0.0033) when compared to uninfected *Muc5ac*$^{-/-}$ mice. Interestingly, at both time points, Hp infected *Muc5ac*$^{-/-}$ mice had significantly lower median corpus mucous metaplasia scores as compared to Hp infected WT mice (Figure 3B, D) (16 wpi &32 wpi; P=0.0057 and P=0.0016, respectively). There was an overall age- related increase in background inflammation and associated changes like atrophy and metaplasia in uninfected WT and *Muc5ac*$^{-/-}$ mice at 32 wpi as compared to 16wpi, as reflected by the increased median GHAI scores at 32 wpi (Figure 3A, C).

Immunohistochemical analysis of mucins and trefoil factors in the gastric corpus of WT and *Muc5ac*$^{-/-}$ mice and its correlation with *Hp* infection

As shown in Figure 4A, strong Muc5ac immunopositivity was observed primarily in the surface and foveolar epithelial pits of the gastric corpus of uninfected WT stomach, with infrequent staining of the glandular neck region. The corpus of *Muc5ac*$^{-/-}$ mice, as expected, did not show any specific Muc5ac immunostaining, although mild non-specific background was observed within the epithelial stroma (Figure 4B). Muc5ac immunopositivity was seen in the apical foveolar pits of uninfected WT stomach and there was also a reduction in Muc5ac staining within foveolar pits of the gastric corpus overlying hyperplastic and mucous metaplastic regions of *Hp*-infected WT mice (Figure 4C, D). Muc1 was highly expressed in foveolar pits and also moderately within deeper glands of the gastric corpus in both uninfected WT and *Muc5ac*$^{-/-}$ mice (Figure 4E). In *Hp*-infected WT and *Muc5ac*$^{-/-}$ mice, Muc1 immunostaining was seen prominently within most hyperplastic foveolar and glandular regions (Figure 4E,G) but was frequently reduced in areas of mucous metaplasia especially in the corpus of WT *Hp*-infected stomachs (Figure 4H).

Trefoil factors are closely associated with gastric mucosal biology, as determined by the ability of TFF1 to bind to MUC5AC (24) and by the increased expression of TFF2 in Spasmolytic Polypeptide Expressing Metaplasia (SPEM) (21). In both uninfected WT and *Muc5ac*$^{-/-}$ mice (Figure 5A–D), Tff1 staining was primarily restricted to corpus surface foveolar epithelium. In Hp infected WT and *Muc5ac*$^{-/-}$ mice there was a slight reduction in Tff1 immunoreactivity in areas where the metaplastic changes extended up to the surface epithelium. Tff2 expression in the WT uninfected stomach was observed within mucous neck cells of the corpus (Figure 5E–H), basal aspects of antral/pyloric glands and within duodenal Brunner's glands (shown in Figure 3). The corpus of uninfected *Muc5ac*$^{-/-}$ mice (Figure 5F, H) showed similar Tff2 expression patterns as seen in the WT uninfected stomach. In both the infected WT and *Muc5ac*$^{-/-}$ stomachs, there was an aberrant increase of Tff2 immunoreactivity within metaplastic (mucous and pseudopyloric types of metaplasia) and hyperplastic glands of the corpus (Figure 5G, H).

GSII Lectin and Clusterin immunostaining confirms that gastric mucous metaplasia is inhibited in *Hp*-infected *Muc5ac*$^{-/-}$ mice compared to WT *Hp*-infected mice

We used Clusterin and GSL II immunostaining to characterize the gastric metaplasia observed in both WT and *Muc5ac*$^{-/-}$ Hp-infected mice. The lectin, *Griffonia simplicifolia*

(*GSL II*), is a well characterized marker of mucin and it labels the corpus neck cells and antral basal glands (21). GSL II staining is increased following *Hp* infection in response to loss of oxyntic cells and expansion and/or transformation to mucous metaplasia (21). In our study, GSL II lectin staining was restricted to a thin layer of corpus mucous neck cells in uninfected mice (Figure 6, rectangular boxes), but was prominently increased in areas of corpus metaplasia following *Hp* infection in both WT and *Muc5ac$^{-/-}$* mice (Figure 6, middle and bottom panels). Interestingly, in metaplastic regions, the expression of GSII expanded from the neck region into the hyperplastic foveolar epithelium as well as deep into the basal aspect of mucosa where chief cells are normally located. Within *Hp*-infected groups, gastric corpus GSL II lectin staining was more extensive and intense in the WT mice as compared to *Muc5ac$^{-/-}$* and this correlated with higher levels of mucous metaplasia observed in the *Hp*-infected WT group (Figure 6, bottom panels). GSL II labelling was also observed in a proportion of glands classified as pseudopyloric metaplasia on the basis of the typical morphology of these metaplastic tubules lacking a mucous filled cytoplasmic appearance (Figure 6 and Figure 3G, H).

SPEM is a preneoplastic metaplastic phenotype that is relevant in mouse gastric cancer models. Mice do not typically manifest intestinal metaplasia as noted in humans during the Correa stepwise cascade of gastric carcinogenesis (31). Clusterin is a recently identified marker of SPEM in murine models (31) and we sought to explore its expression levels within the different experimental groups. Clusterin labelling was mostly absent or sparse within the gastric corpus epithelium of both the uninfected WT and *Muc5ac$^{-/-}$* mice, but was prominently observed multifocally within the metaplastic glands of the Hp-infected WT and *Muc5ac$^{-/-}$* mice (Figure 7). However, the degree of Clusterin positivity within glands was variable depending upon the type of metaplasia (i.e. pseudopyloric metaplasia vs mucous metaplasia or mixed forms). A strong positivity for Clusterin was noted in a significant proportion of metaplastic glands of pseudopyloric type, and only infrequently observed within glands of the mucous metaplasia type (Figure 7). This correlated with an appreciable decrease in overall clusterin staining (SPEM transformation) in WT infected stomachs in which mucous metaplasia was more prominent as compared to infected *Muc5ac$^{-/-}$* mice.

Gastric *Hp* colonization dynamics in WT and *Muc5ac$^{-/-}$* mice

At 16 wpi, the levels of gastric *H. pylori*, as measured by qPCR in both male and female *Muc5ac$^{-/-}$* mice, were significantly (P<0.045) higher than their male and female WT counterparts (Figure 8). Additionally, the levels of gastric *Hp* in male *Muc5ac$^{-/-}$* male mice were significantly higher than female *Muc5ac$^{-/-}$* mice at 16 wpi but the differences were not statistically significant between infected WT males and WT females. At 32 wpi, there was no significant difference in gastric *Hp* levels between genotypes or genders.

Hp associated gastric gene expression

Gastric cytokines, including *Tnfα, Ifnγ, Il-1β, Il-17A, Il-22*, and *Il-10* have been shown to play an important role in influencing histological manifestations of *Hp* infection. In general, infected mice had significantly higher mRNA levels of these cytokines compared to genotype-matched uninfected mice (P<0.05). The *H. pylori*- associated increase in *Tnfα*

mRNA levels in $Muc5ac^{-/-}$ mice were significantly lower than that of gender-matched WT mice at 16 wpi (p= 0.017 & p= 0.036, male and female respectively) and 32 wpi- males only, P=0.025). Additionally, there was significantly lower gastric $Il-17A$ mRNA levels at 16 wpi in infected $Muc5ac^{-/-}$ males (P=0.025) compared to their Hp infected WT counterparts. The mRNA levels of gastric $Ifn\gamma$, $Il-1\beta$, $Il-10$ and $Il-22$ did not show any significant differences between the infected genotypes. Trefoil factor 2 ($Tff2$), another marker for SPEM was comparable among the groups (Figures 9, panels 1 & 2) though there was an enhancement of gastric Tff2 positive areas in infected mice as compared to the uninfected mice in both genotypes (Figure 5 E–H).

DISCUSSION

This study was designed to elucidate the role of Muc5AC in Hp pathogenesis utilizing $Muc5ac^{-/-}$ mice in a well-established chronic Hp infection murine model. Our results have illustrated several interesting observations. First, $Muc5ac^{-/-}$ mice are spontaneously predisposed to develop an Hp independent gastric phenotype of antro-pyloric inflammation, hyperplasia and dysplasia, including development of adenomas. Further, Muc5ac$^{-/-}$ mice, in general, have slightly attenuated Hp induced corpus pathology compared to WT mice, in particular a significant reduction in oxyntic mucous metaplasia. At the cytokine level, most notable in males, gastric TNFa and IL-17A levels were significantly higher in Hp infected WT B6–129 mice as compared to infected $Muc5ac^{-/-}$ mice, which correlated with previously observed trends for these cytokines in mouse models of Hp associated gastritis (19, 20, and 21). Interestingly, $Muc5ac^{-/-}$ mice (predominantly males) during the initial course of infection (16 wpi) displayed significantly higher gastric Hp colonization levels and an associated significant reduction in gastric corpus mucous metaplasia compared to Hp-infected WT mice, but these differences in colonization levels were not noted at the end of the study (32 wpi).

Trefoil factors are small secreted proteins in mammals that share a conserved trefoil domain of 42–43 amino acids in humans (TFF1, TFF2 and TFF3) and their homologues (Tff1, Tff2 and Tff3) in mice (5, 9, 24–27). In the stomach, TFF1, also known as ps2/TFF1, is expressed in the superficial foveolar epithelium of the human corpus and antrum and binds to MUC5AC, the primary mucin in this location (24). TFF1 interacts with both the gastric MUC5AC and intestinal MUC2 through their von Willebrand factor C (VWFC) cysteine rich domains, and this interaction is largely responsible for the gastro-intestinal protective effect of TTF1 (27). In biopsies from children, it was also shown that TFF1 co-localized with Hp in the superficial mucous layer of the surface epithelium and within pits of the gastric mucosa, thus mimicking the localization of MUC5AC (24, 28). The deficiency of Tff1 in mice has been reported to cause the development of spontaneous antro-pyloric adenomas and carcinoma (29). TFF2 is expressed in the mucous neck cells in the fundus or corpus, in the basal glands of the antrum and pylorus and in Brunner's glands of the duodenum (21, 26 32). Mice deficient in Tff2 have accelerated progression to premalignant dysplasia in the antrum/pylorus of Hp-infected mice (21). In contrast, TFF3 is not expressed in the stomach but elaborated primarily by goblet cells in the intestinal tract (25, 26). Thus, the expression pattern of TFF1 and TFF2 mimics those of MUC5ac/MUC1 and MUC6,

respectively, in normal stomach of humans and mice, as well as in human gastric carcinoma patients and in mouse models (7–9, 21, 25, 28, and 32).

Our findings of spontaneous antro-pyloric proliferative lesions in uninfected $Muc5ac^{-/-}$ mice is similar in some respects to the spontaneous antro-pyloric lesions observed in an earlier study with $Tff1^{-/-}$ (pS2) mice on a similar C57BL/6 background (29). We observed spontaneous antro-pyloric hyperplasia and dysplasia in nearly 70% of $Muc5ac^{-/-}$ mice housed in two different institutions (NIEHS and MIT) at about 9–10 months of age with at least 17% of mice developing adenomas but no carcinomas were noted. However, in the earlier study by Lefebvre, the antro-pyloric dysplastic lesions were more rapid and severe, with 100% penetrance affecting both $Tff1^{-/-}$ sexes equally and progressed to antral carcinoma (30%) at about 5 months of age (29). Of interest, we observed strong expression of Tff1 within the antral/pyloric hyperplastic/adenomatous glands of $Muc5ac^{-/-}$ mice. This suggests that Tff1 was unaffected from the deficiency of $Muc5ac^{-/-}$ and it likely did not play a key role in the development of spontaneous antro-pyloric proliferative lesions in $Muc5ac^{-/-}$ mice. The $Tff1^{-/-}$ mice used in the earlier study (29) were not assessed for Muc5ac expression levels, and hence our data raises the possibility of Muc5ac downregulation in $Tff1^{-/-}$ mice as a co-contributor in antro-pyloric carcinogenesis. In a manner similar to $Muc5ac^{-/-}$ mice, $A4gnt^{-/-}$ mice that are deficient in the gastric αGlcNAc-terminated glandular mucin are also prone to pyloric carcinogenesis via a hyperplasia-dysplasia-neoplasia pathway (33), thus implying that alterations in gastric mucins either in the surface or within glands region predisposes to pyloric tumors. Interestingly, one of the adenomas in the gastric antro-pyloric region of $Muc5ac^{-/-}$ mice also showed well demarcated foci with histomorphological features of presumptive neuroendocrine differentiation; however, it was not positive for ChrgA, unlike the typical expected findings of tissue ChrgA positivity with frequent elevated plasma levels of ChrgA of human patients with gastric neuroendocrine tumors or carcinoids (30). In humans, gastric neuroendocrine tumors (GNETs), also called gastric carcinoids, constitute less than 2% of all gastric neoplasms and are mainly derived from enterochromaffin-like (ECL) cells in the glands of the gastric mucosa. They can be solitary or multiple tumors, rarely metastatic and are often diagnosed as an incidental finding with or without overt clinical symptoms. The incidence of GNETs has increased in recent decades and is attributed to increased awareness, screening, and diagnosis via upper gastrointestinal endoscopy (30).

The relevance of these Hp independent antro-pyloric spontaneous tumors in the absence of Muc5ac needs further exploration for its translational significance in humans. Nevertheless, these lesions in terms of location mimic rare instances of human pyloric gland adenomas located in the gastric outlet (34). Although cancers have been reported in association with gastric hyperplastic polyps in humans, these are extremely rare (35). Unlike foveolar gland adenomas, where cells have an apical mucous cap and express MUC5AC in humans, pyloric gland adenomas typically do not have cells with a distinct mucin cap and tend to label with both MUC5AC and MUC6 and pose a risk for progression to carcinoma (34). Gastric hyperplastic polyps are infrequently detected in human endoscopies and can be single (predominant) or multiple, and are more common in females than males. The polyps may be flat, sessile or pedunculated with a histological spectrum of fundic gland polyps, hyperplastic polyps and adenomatous polyps (35). Gastric polyps are increasingly

recognized in middle aged humans and their distribution is now altered from its predominant antral location in past descriptions to favor a more corpus location (35). Large antral polyps or adenomas in humans can lead to gastric outlet obstruction and associated clinical symptoms (35).

The corpus gastric histopathological index scores in *Hp*-infected WT and *Muc5ac*−/− mice at 16 wpi and 32 wpi trended in a manner similar to that of historical data in C57B/6–129 mice (19, 21) and with significantly higher scores than their respective uninfected controls. A comparison of the two infected groups indicates a trend towards slightly lower overall gastric pathology index and importantly a significant reduction in mucous metaplasia in *Hp*-infected *Muc5ac*−/− mice. Oxyntic metaplastic changes in mice following Hp infection are not typical of intestinal metaplasia seen in *Hp* infected humans and more often are a combination of mucous metaplasia and pseudopyloric metaplasia, both of which express markers of SPEM (21, 22, 25). Mucous metaplasia can occur spontaneously and independent of Hp infection (21, 22) but we have also frequently observed its enhancement following Hp infection (19, 20, 21). Given the importance of Muc5ac in mucin/mucous formation, we consider mucous metaplasia, though murine-specific, to be an important parameter to include in our analysis as it also shares many features of the molecular aspects of SPEM noted in pseudopyloric metaplasia. In WT *Hp* infected mice, in areas with corpus oxyntic changes, particularly with mucous metaplasia, there was a decrease in Muc5ac immunostaining of the overlying foveolar epithelial surface pits. In the same WT *Hp* infected mice, Muc5ac staining was enhanced within hyperplastic regions of the antrum and this corresponds to altered Muc5ac expression profile observed in *Hp* - infected patients (8, 9, 26).

Our results from GSL II and Clusterin immunohistochemistry has shown that SPEM occurs in a significant proportion of glands characterized morphologically as pseudopyloric metaplasia. It also occurs to a certain extent in glands undergoing mucous metaplasia and it is likely that the presence of Muc5ac aids in an unidentified manner to transformation of oxyntic cells to mucous metaplasia phenotype. Recently, it was shown using Muc1 deficient mice that MUC1 protects against *Hp* induced gastric pathology mice by regulation of the NLRP3 inflammasome (36); however, we noted strong expression of Muc1 in *Hp*-infected corpus and within spontaneous antral adenomas of *Muc5ac*−/− mice. Tff2, which is a marker for SPEM and binds to MUC6 (37), was shown to be highly expressed in metaplastic (both mucous and pseudopyloric type) gastric corpus of *Hp*-infected WT and *Muc5ac*−/− groups which is in agreement with our earlier findings in the corpus of *Hp*-infected wild type mouse stomach (21). In our previous study in *Tff2*−/− mice, there was strong evidence for a protective role by Tff2 in *Hp* induced IFN-γ associated gastric corpus pathology (6 months of age) and late onset (19 months of age) antral carcinogenesis (21). In this study, the antral proliferative lesions strongly expressed Tff2 and there was no difference in *Tff2* gene expression levels on the basis of qPCR data across all experimental groups.

The inflammatory gastric pathology in *Hp*-infected WT and *Muc5ac*−/− mice correlated with an increase in cytokines, including *Tnfa, Ifnγ, Il-1β, Il-17A,* and *Il-22,* as previously documented (19, 20, 21). However, *Tnfa* at both post-infection time points and *Il-17A* at 16 wpi (males only) was significantly reduced in the stomach of *Hp* Muc5ac−/−mice as

compared to their *Hp*-infected WT, whereas there was no significant difference in *Ifnγ* levels between the two infected groups. This contrasts the documented significant increase in gastric *Ifnγ* levels in *Hp*-infected *Tff2$^{-/-}$* mice on a C57BL/6 background (21). We also observed significantly enhanced *Hp* gastric colonization levels in *Muc5ac$^{-/-}$* mice at 16 wpi, although the colonization levels were similar in *Muc5ac$^{-/-}$* and WT mice at 32wpi. Previous data with *Hp* infection studies in WT C57BL/6 have shown either an inverse correlation between grade of inflammation and colonization density (20, 21), or a lack of any significant correlation between inflammation and *Hp* colonization in C57BL/6 mice (39) or *Tff2$^{-/-}$* C57BL/6 mice (21), respectively. In C57BL mouse studies with the gastric *H. pylori* and entero-hepatic *H. bilis* (19) or *H. muridarum* (20), it was shown that *H. bilis* or *H. muridarum* intestinal colonization was associated with a significant attenuation of *Hp* induced gastric pathology in a setting of higher *Hp* gastric colonization levels. It was hypothesized that the inhibitory effect was likely mediated due to anti-inflammatory effects of regulatory T (Foxp3$^+$ T$_{REG}$) cells (20, 21). It is also possible that the underlying reason for this enhancement of *Hp* colonization in *Muc5ac$^{-/-}$* mice at 16wpi is linked to the inherent ability of *Hp* to impair mucin production and turnover (38) which might be more pronounced in the absence of Muc5ac, thus leading to reduced bacterial clearance and enhanced *Hp* adherence. Muc1, another gastric epithelial surface mucin was shown to play a beneficial role in a mouse model of *Hp* infection by blocking downstream activation of nuclear factor-κB inflammatory signaling pathway (36). Further, *Hp*-infected *Muc1$^{-/-}$* mice showed significantly enhanced gastric *Hp* colonization, coupled with increased tissue transcript levels of TNF-α and keratinocyte chemoattractant (KC) (40). Interestingly, in our study, in *Muc5ac$^{-/-}$* mice, enhanced *Hp* gastric colonization was observed in the setting of attenuated inflammation and reduced *Tnfα* tissue levels, raising the possibility that Muc5ac may enhance bacterial clearance and limit persistent colonization within deeper glands, while at the same time serving as a critical receptor for *Hp*, activating downstream signaling cascades and host immune responses.

In conclusion, we have shown that *Muc5ac$^{-/-}$* mice are predisposed to the development of spontaneous antro-pyloric proliferative lesions, and could serve as a useful model to study antro-pyloric proliferative dysplastic lesions. In addition, *Hp* infection is mildly attenuated in the absence of Muc5ac in tandem with a reduction in gastric Il17a and/or Tnf-α expression. Further studies are needed to clarify the roles of Muc5ac in *Hp* colonization and adherence mechanisms, as well to explore the interaction between Muc5ac and other innate local factors in maintaining gastric homeostasis.

Supplementary Material

Refer to Web version on PubMed Central for supplementary material.

ACKNOWLEDGEMENTS:

REFERENCES:

1. Moore ME, Boren T, Solnick JV. Life at the margins: modulation of attachment proteins in *Helicobacter pylori*. Gut Microbes 2011;2:42–46. [PubMed: 21637017]

2. Oleastro M, Menard A. The Role of *Helicobacter pylori* Outer Membrane Proteins in Adherence and Pathogenesis. Biology (Basel) 2013;2:1110–1134. [PubMed: 24833057]

3. Juge N Microbial adhesins to gastrointestinal mucus. Trends Microbiol 2012;20:30–39. [PubMed: 22088901]

4. Yandrapu H, Sarosiek J. Protective Factors of the Gastric and Duodenal Mucosa: An Overview. Curr Gastroenterol Rep 2015;17:24. [PubMed: 26109006]

5. Kemmerly T, Kaunitz JD. Gastroduodenal mucosal defense. Curr Opin Gastroenterol 2013;29:642–649. [PubMed: 24100725]

6. Hasnain SZ, Gallagher AL, Grencis RK, Thornton DJ. 2013. A new role for mucins in immunity: insights from gastrointestinal nematode infection. Int J Biochem Cell Biol 2013;45:364–374. [PubMed: 23107603]

7. Schmitz JM, Durham CG, Ho SB, Lorenz RG. Gastric mucus alterations associated with murine *Helicobacter* infection. J Histochem Cytochem 2009;57:457–467. [PubMed: 19153195]

8. Babu SD, Jayanthi V, Devaraj N, Reis CA, Devaraj H. 2006 Expression profile of mucins (MUC2, MUC5AC and MUC6) in *Helicobacter pylori* infected preneoplastic and neoplastic human gastric epithelium. Mol Cancer 2006;5:10. [PubMed: 16545139]

9. Machado JC, Nogueira AM, Carneiro F, Reis CA, Sobrinho-Simões M. Gastric carcinoma exhibits distinct types of cell differentiation: an immunohistochemical study of trefoil peptides (TFF1 and TFF2) and mucins (MUC1, MUC2, MUC5AC, and MUC6). J Pathol 2000;190:437–443. [PubMed: 10699992]

10. Park JS, Yeom JS, Seo JH, Lim JY, Park CH, Woo HO, et al. Immunohistochemical Expressions of MUC2, MUC5AC, and MUC6 in Normal, *Helicobacter pylori* Infected and Metaplastic Gastric Mucosa of Children and Adolescents. Helicobacter 2015;20:260–268. [PubMed: 25704078]

11. Liu C, Smet A, Blaecher C, Flahou B, Ducatelle R, Linden S, Haesebrouck F. Gastric de novo Muc13 expression and spasmolytic polypeptide-expressing metaplasia during *Helicobacter heilmannii* infection. Infect Immun 2014;82:3227–3239. [PubMed: 24866791]

12. Teixeira A, David L, Reis CA, Costa J, Sobrinho-Simões M. Expression of mucins (MUC1, MUC2, MUC5AC, and MUC6) and type 1 Lewis antigens in cases with and without *Helicobacter pylori* colonization in metaplastic glands of the human stomach. J Pathol 2002;197:37–43. [PubMed: 12081201]

13. Boltin D, Niv Y. Mucins in Gastric Cancer - An Update. J Gastrointest Dig Syst 2013;3:15519. [PubMed: 24077811]

14. Schreiber S, Konradt M, Groll C, Scheid P, Hanauer G, Werling HO, et al. The spatial orientation of *Helicobacter pylori* in the gastric mucus. Proc Natl Acad Sci U S A 2004;101:5024–5029. [PubMed: 15044704]

15. Lindén SK, Wickström C, Lindell G, Gilshenan K, Carlstedt I. Four modes of adhesion are used during *Helicobacter pylori* binding to human mucins in the oral and gastric niches. Helicobacter 2008;13:81–93. [PubMed: 18321298]

16. Borén T, Falk P, Roth KA, Larson G, Normark S. Attachment of *Helicobacter pylori* to human gastric epithelium mediated by blood group antigens. Science 1993;262:1892–1895. [PubMed: 8018146]

17. Dunne C, Dolan B, Clyne M. Factors that mediate colonization of the human stomach by *Helicobacter pylori*. World J Gastroenterol 2014;20:5610–5624. [PubMed: 24914320]

18. Van de Bovenkamp JH, Mahdavi J, Korteland-Van Male AM, Büller HA, Einerhand AW, Borén T, et al. The MUC5AC glycoprotein is the primary receptor for *Helicobacter pylori* in the human stomach. Helicobacter 2003;8:521–532. [PubMed: 14535999]

19. Lemke LB, Ge Z, Whary MT, Feng Y, Rogers AB, Muthupalani S, Fox JG. Concurrent *Helicobacter bilis* infection attenuates proinflammatory *H. pylori* induced gastric pathology. Infect Immun 2009; 77: 2147–2158. [PubMed: 19223483]

20. Ge Z, Feng Y, Muthupalani S, Eurell LL, Taylor NS, Whary MT, Fox JG. Coinfection with Enterohepatic *Helicobacter* species can ameliorate or promote *Helicobacter pylori*-induced gastric pathology in C57BL/6 mice. Infect Immun 2011;79:3861–3871. [PubMed: 21788386]

21. Fox JG, Rogers AB, Whary MT, Ge Z, Ohtani M, Jones EK, Wang TC. Accelerated progression of gastritis to dysplasia in the pyloric antrum of TFF2 −/− C57BL6 x Sv129 *Helicobacter pylori*-infected mice. Am J Pathol 2007;171:1520–1528. [PubMed: 17982128]

22. Rogers AB. Histologic scoring of gastritis and gastric cancer in mouse models. Methods Mol Biol 2012;921:189–203. [PubMed: 23015505]

23. Jae Kyu Sung. Diagnosis and management of gastric dysplasia. Korean J intern Med. 2016; 31:201–209. [PubMed: 26932397]

24. Ruchaud-Sparagano MH, Westley BR, May FE. The trefoil protein TFF1 is bound to MUC5AC in human gastric mucosa. Cell Mol Life Sci 2004;61:1946–1954. [PubMed: 15289936]

25. Matsuda K, Yamauchi K, Matsumoto T, Sano K, Yamaoka Y, Ota H. Quantitative analysis of the effect of Helicobacter pylori on th.e expressions of SOX2, CDX2, MUC2, MUC5AC, MUC6, TFF1, TFF2, and TFF3 mRNAs in human gastric carcinoma cells. Scand J Gastroenterol 2008;43:25–33. [PubMed: 18938748]

26. Taupin D, Podolsky DK. Trefoil factors: initiators of mucosal healing. Nat Rev Mol Cell Biol 2003;4:721–732. [PubMed: 14506475]

27. Tomasetto C, Masson R, Linares JL, Wendling C, Lefebvre O, Chenard MP, et al. pS2/TFF1 interacts directly with the VWFC cysteine-rich domains of mucins. Gastroenterology 2000;118:70–80. [PubMed: 10611155]

28. Clyne M, Dillon P, Daly S, O'Kennedy R, May FE, Westley BR, et al. H*elicobacter pylori* interacts with the human single-domain trefoil protein TFF1. Proc Natl Acad Sci U S A 2004;101:7409–7414. [PubMed: 15123808]

29. Lefebvre O, Chenard MP, Masson R, Linares J, Dierich A, LeMeur M, et al. Gastric mucosa abnormalities and tumorigenesis in mice lacking the pS2 trefoil protein. Science 1996;274:259–262. [PubMed: 8824193]

30. Christopoulos C, Papavassiliou E. (2005) Gastric neuroendocrine tumors: Biology and management Vol. 18, Annals of Gastroenterology, 127–140.

31. Choi E, Hendley AM, Bailey JM, Leach SD, Goldenring JR.. Expression of Activated Ras in Gastric Chief Cells of Mice Leads to the Full Spectrum of Metaplastic Lineage Transitions. Gastroenterology 2016;150:918–930 e913. [PubMed: 26677984]

32. Xia HH, Yang Y, Lam SK, et al. Aberrant epithelial expression of trefoil family factor 2 and mucin 6 in *Helicobacter pylori* infected gastric antrum, incisura, and body and its association with antralisation. J Clin Pathol 2004;57:861–866. [PubMed: 15280409]

33. Karasawa F, Shiota A, Goso Y, Kobayashi M, Sato Y, Masumoto J, et al. Essential role of gastric gland mucin in preventing gastric cancer in mice. The Journal of clinical investigation. 2012;122(3):923–34. [PubMed: 22307328]

34. Pezhouh MK, Park JY. Gastric pyloric gland adenoma. Arch Pathol Lab Med 2015;139:823–826. [PubMed: 26030253]

35. Markowski AR, Markowska A, Guzinska-Ustymowicz K. Pathophysiological and clinical aspects of gastric hyperplastic polyps. World J Gastroenterol.2016; 22(40):8883–8891. [PubMed: 27833379]

36. Ng GZ, Menheniott TR, Every AL, Stent A, Judd LM, Chionh YT, et al. The MUC1 mucin protects against *Helicobacter pylori* pathogenesis in mice by regulation of the NLRP3 inflammasome. Gut 2016;65:1087–1099. [PubMed: 26079943]

37. Hoffmann W TFF2, a MUC6-binding lectin stabilizing the gastric mucus barrier and more (Review). Int J Oncol 2015;47:806–816. [PubMed: 26201258]

38. Navabi N, Johansson ME, Raghavan S, Lindén SK. *Helicobacter pylori* infection impairs the mucin production rate and turnover in the murine gastric mucosa. Infect Immun 2013;81:829–837. [PubMed: 23275091]

39. Thompson LJ, Danon SJ, Wilson JE, O'Rourke JL, Salama NR, Falkow S, et al. Chronic *Helicobacter pylori* infection with Sydney strain 1 and a newly identified mouse-adapted strain

(Sydney strain 2000) in C57BL/6 and BALB/c mice. Infect Immun 2004;72:4668–4679. [PubMed: 15271928]

40. Guang W, Ding H, Czinn SJ, et al. Muc1 cell surface mucin attenuates epithelial inflammation in response to a common mucosal pathogen. J Biol Chem 2010;285:20547–20557. [PubMed: 20430889]

A   Pathology Index- 16wpi

B   Pathology Index- 32 wpi

C   Dysplasia- 16wpi
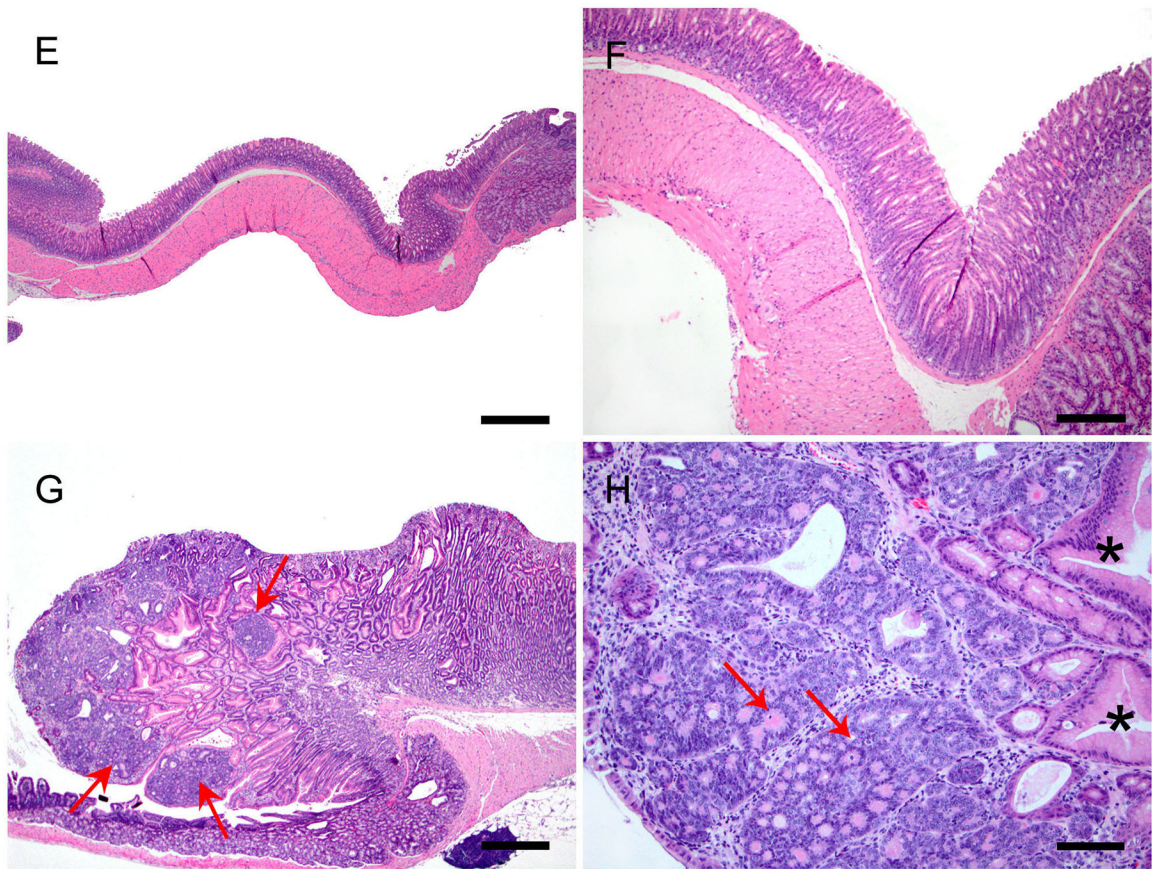
D   Dysplasia- 32wpi

Figure 1: Gastric antro-pyloric spontaneous pathology in *Muc5ac*$^{-/-}$ mice:
Cumulative antrum/pylorus pathology index scores in the different groups of mice at 16 wpi
(A) and 32 wpi (B). Antro-pyloric dysplasia score chart for different groups of mice at 16
wpi (C) and 32 wpi (D). (*) = p<0.05, (**) = p<0.01, (***) = p<0.001, Uninf-Uninfected,
Hp- Hp-infected. E-F: Representative H&E images of the uninfected gastric antrum/pylorus
at 32 wpi time point. E. WT uninfected, low mag, normal. F. WT uninfected, high mag,
normal. G. *Muc5ac*$^{-/-}$ uninfected, (low mag) showing a large pyloric adenoma with
multinodular (arrows) pleomorphic appearance. H. *Muc5ac*$^{-/-}$ uninfected- Higher
magnification image of the micro nodules within the adenoma showing more basophilic
neoplastic cells forming rosettes (neuroendocrine like pattern) adjacent to dysplastic
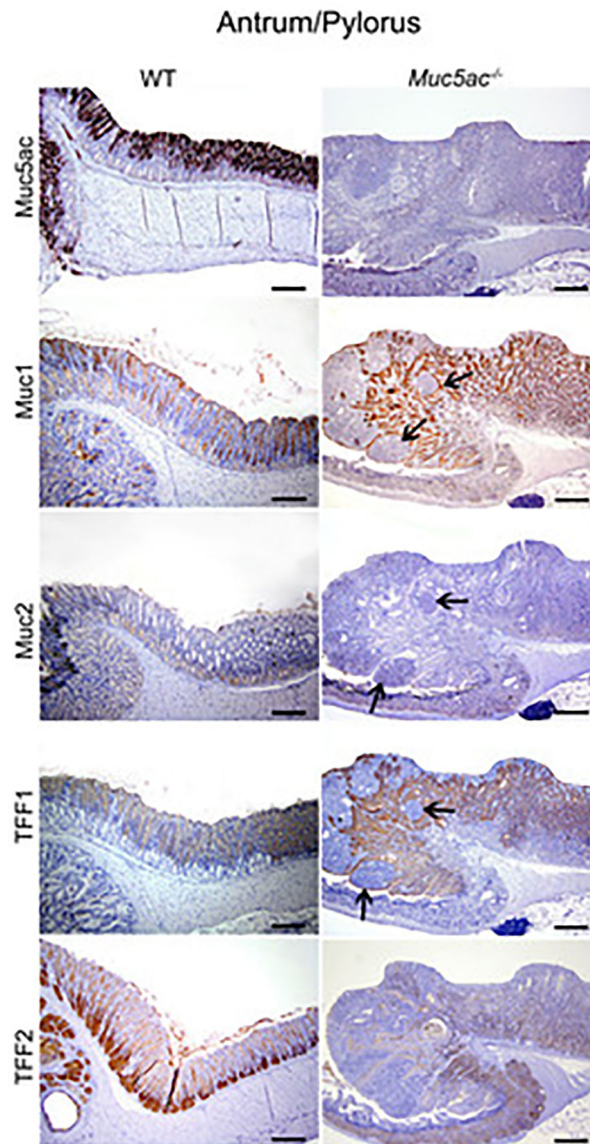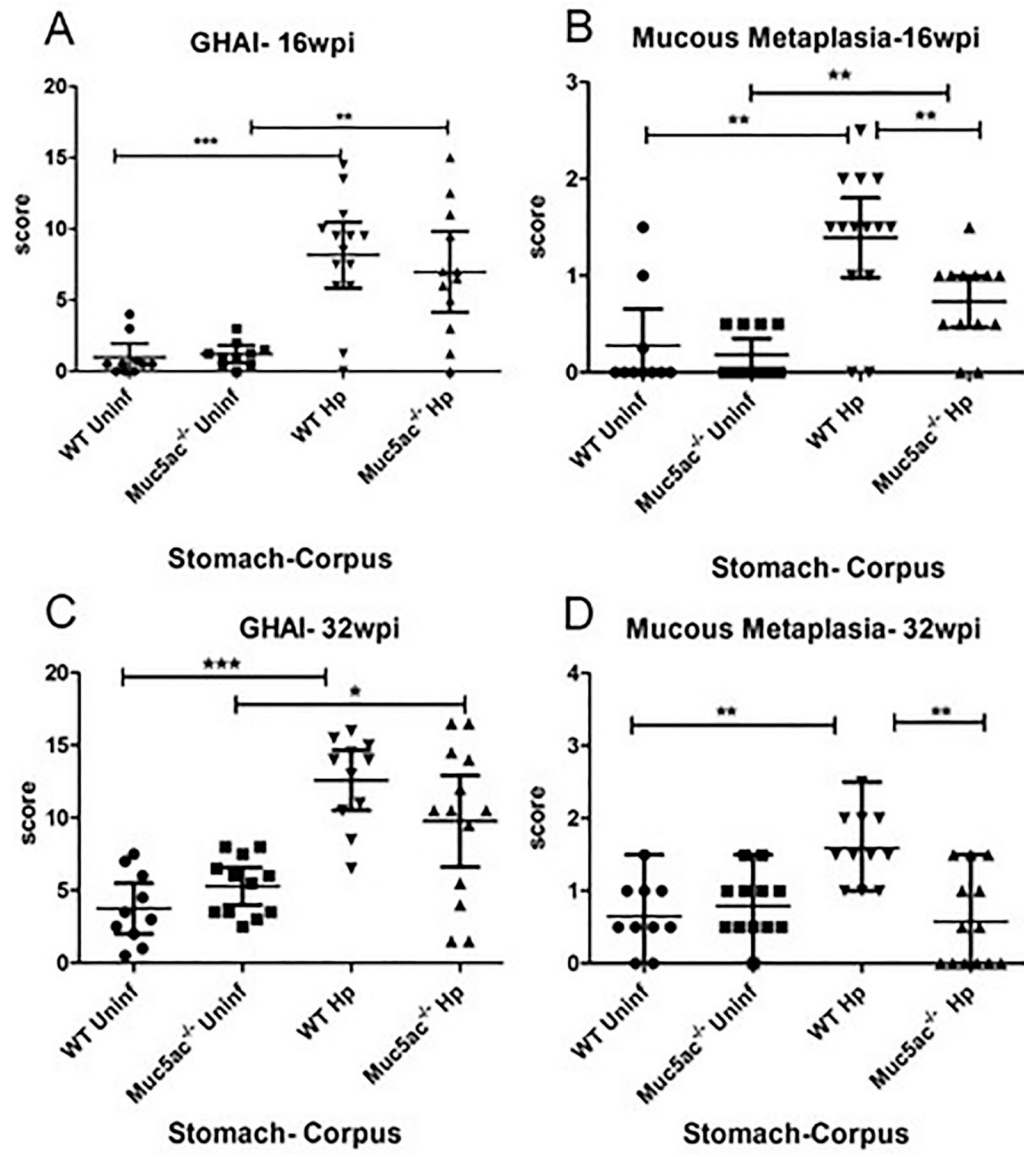glandular epithelium (stars). Bars: A, C- 400μM, B-160μM, D-80μM

Figure 2: Immunohistochemical analysis of the antrum/pylorus for various mucins and trefoil factors:

Panels shows staining pattern of various markers in normal uninfected WT mice and polypoid adenoma in the antro-pyloric region of uninfected *Muc5ac*$^{-/-}$ mice at 39 weeks of age. Note lack of epithelial Muc5ac and Muc2 staining in *Muc5ac*$^{-/-}$ antrum/pylorus and increased staining intensity for Muc1, TFF2 and TFF2 within the adenoma/hyperplastic antrum/pylorus. Bars: 160μM: All WT images. 400μM: All *Muc5ac*$^{-/-}$ images. Arrows indicate micro adenomas with divergent differentiation within the large adenoma in the pylorus.
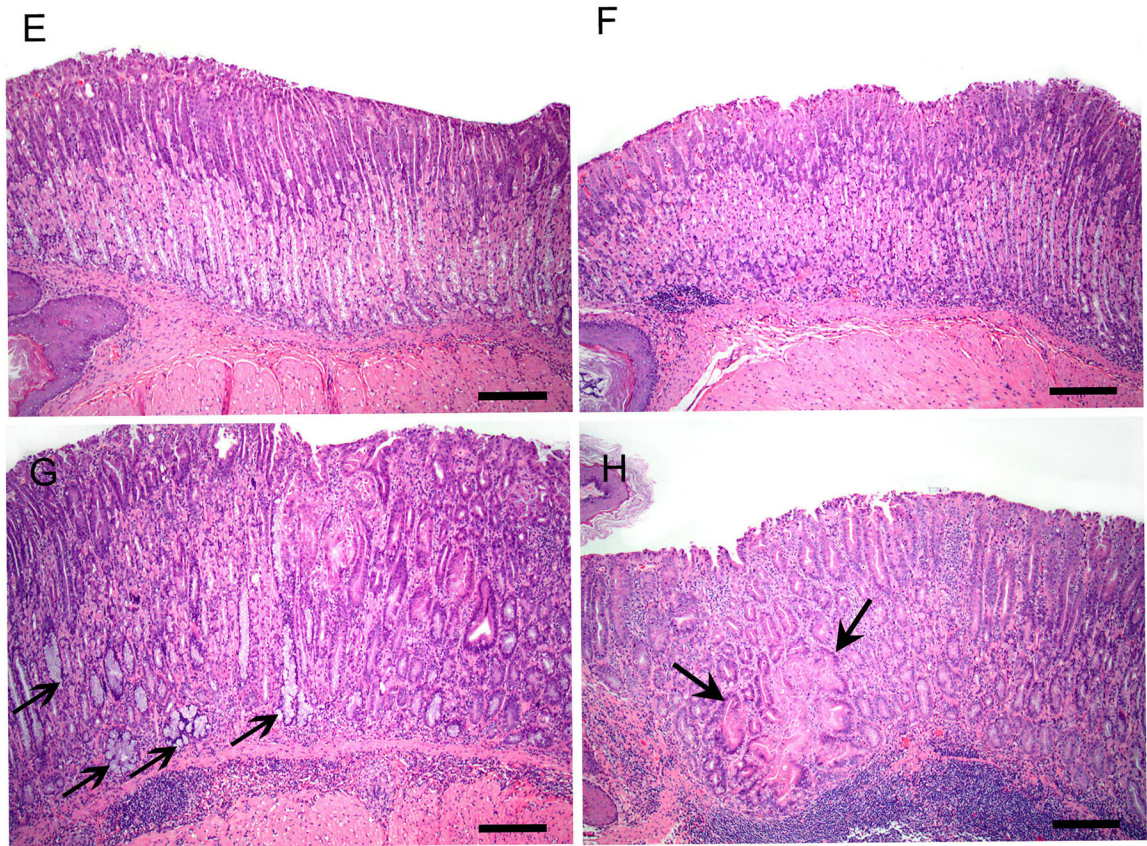
A GHAI- 16wpi

Stomach-Corpus

B Mucous Metaplasia-16wpi

Stomach- Corpus

C GHAI- 32wpi

Stomach- Corpus

D Mucous Metaplasia- 32wpi

Stomach-Corpus

Figure 3: Gastric Corpus pathology in *Hp*-infected WT and *Muc5ac*⁻/⁻ mice:
Charts showing corpus gastric histological activity indices (GHAI) at 16 wpi (A) and 32 wpi (D) and sub-categorical mucous metaplasia scores at 16 wpi (B) and 32 wpi (D). (*) = p<0.05, (**) = p<0.01, (***) = p<0.001. Representative H&E images of the gastric corpus at 32 wpi: E- WT, uninfected; F- *Muc5ac*⁻/⁻, uninfected; G- WT, *Hp*-infected, arrows indicate mucous metaplasia; H- *Muc5ac*⁻/⁻, *Hp*-infected, arrows indicate metaplasia with dysplasia. Bar: 160μM, all images. *Hp* infection in both WT and *Muc5ac*⁻/⁻ gastric corpus showed prominent inflammation, oxyntic loss, metaplasia, hyperplasia and mild dysplasia as compared to their uninfected counterparts with a significant reduction in corpus mucous metaplasia in Hp infected *Muc5ac*⁻/⁻ vs Hp infected WT.
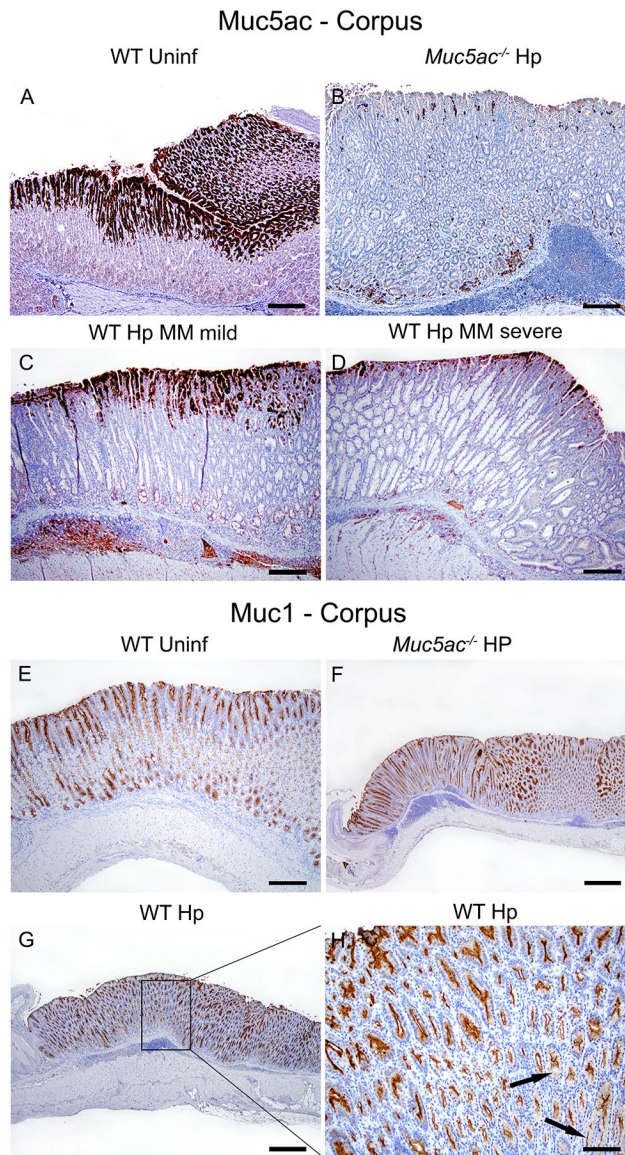
Figure 4: Immunohistochemistry of Muc5ac and Muc1 in the gastric corpus
Muc5ac IHC: A-D, Prominent Muc5ac expression in the gastric foveolar region of the WT
uninfected control (A) and lack of expression in uninfected *Muc5ac*$^{-/-}$ mice at 32 wpi (B).
Muc5ac expression in WT *Hp*-infected stomach in areas of pseudopyloric metaplasia or mild
mucous metaplasia (C, MM mild) compared to a reduction in surface foveolar expression in
areas of severe glandular mucous metaplasia (D, MM severe 32 wpi. Bars: 160μM, All
images Muc1 IHC: E-F: Muc1 expression is robust in the upper 1/3rd and lower 1/3rd of
normal corpus (E, WT uninfected, Bar:160μM) and is enhanced in hyperplastic glands of *Hp*
infected WT and Muc*5ac*$^{-/-}$ gastric corpus (F, G, Bar: 400μM). A slight reduction in
intensity of Muc1 staining in areas of glandular mucous metaplasia (arrows) as shown in the
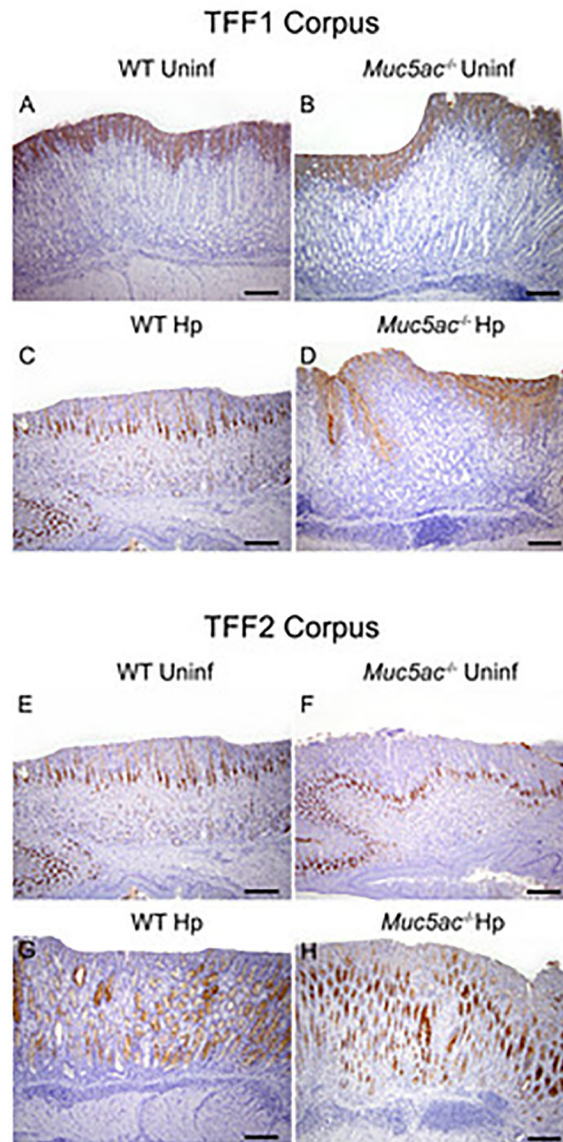higher magnification of inset (H, Bar: 80μM)

TFF1 Corpus

WT Uninf   *Muc5ac-/-* Uninf

A   B

WT Hp   *Muc5ac-/-* Hp

C   D

TFF2 Corpus

WT Uninf   *Muc5ac-/-* Uninf

E   F

WT Hp   *Muc5ac-/-* Hp

G   H

Figure 5: TFF1 and TFF2 Immunohistochemistry in the stomach:
A-D: Tff1 expression is similar in the gastric corpus of both infected and control mice with localization to foveolar pits at 32 wpi. E-F: TFF2 expression is increased in infected animals with strong positivity in metaplastic glands (mucous metaplasia and pseudopyloric type) in both WT and Muc5ac−/− mice at 32 wpi. Bars: 160μM, All images.
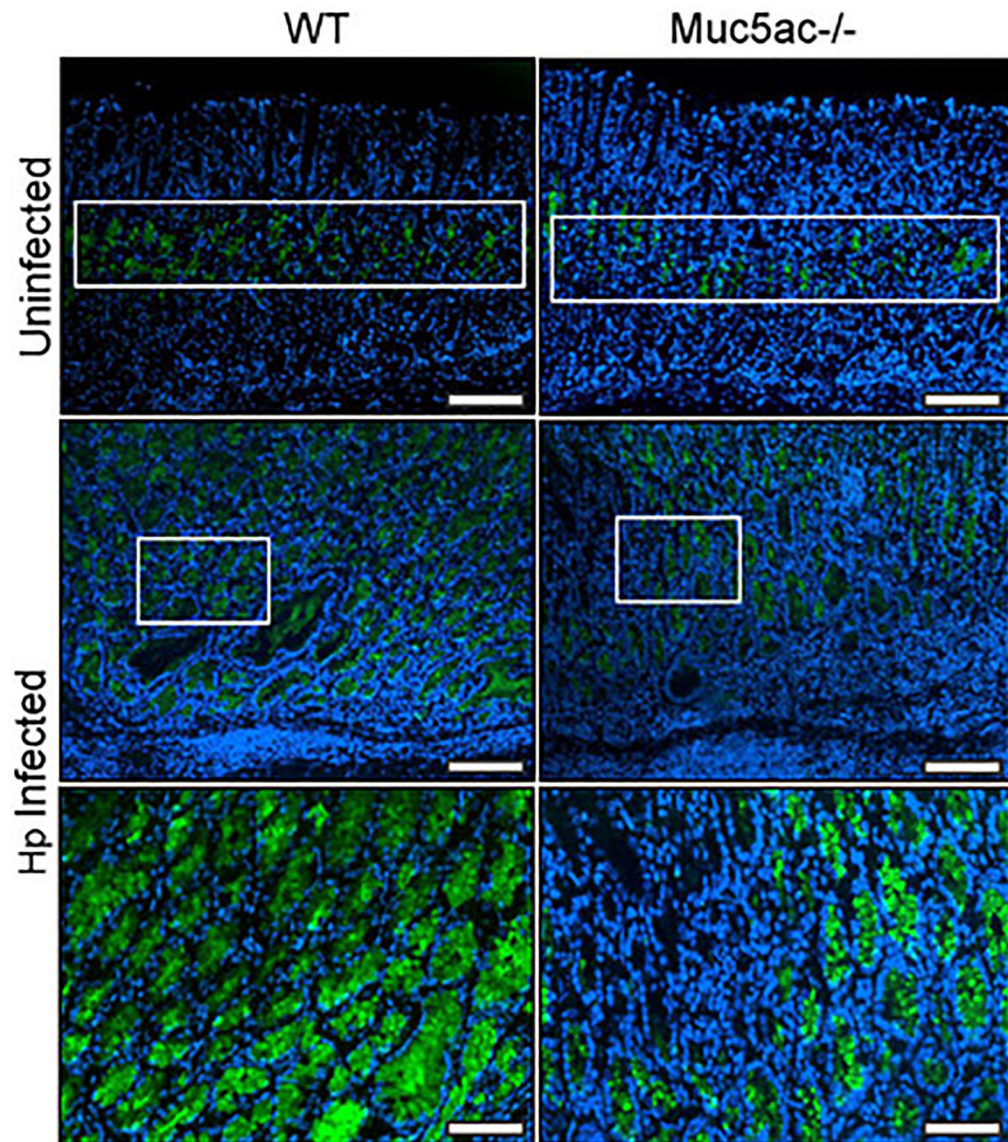
Figure 6: GSL II- Lectin Fluorescent staining in the stomach
In uninfected gastric corpus of WT and *Muc5ac*−/− mice, GSL II fluorescence (FITC, green) was observed within the mucous neck cell region only (white rectangle box) at 32 wpi (top two images). In both the infected groups, there is increased GSL II positive staining throughout the mucosa though in WT corpus (left middle and bottom images), the proportion of glands involved and their intensity of staining is greater than that of *Muc5ac*−/− corpus (right middle and bottom images). Bottom two images are higher magnification images from the boxed square regions. Blue- DAPI nuclear counter stain.
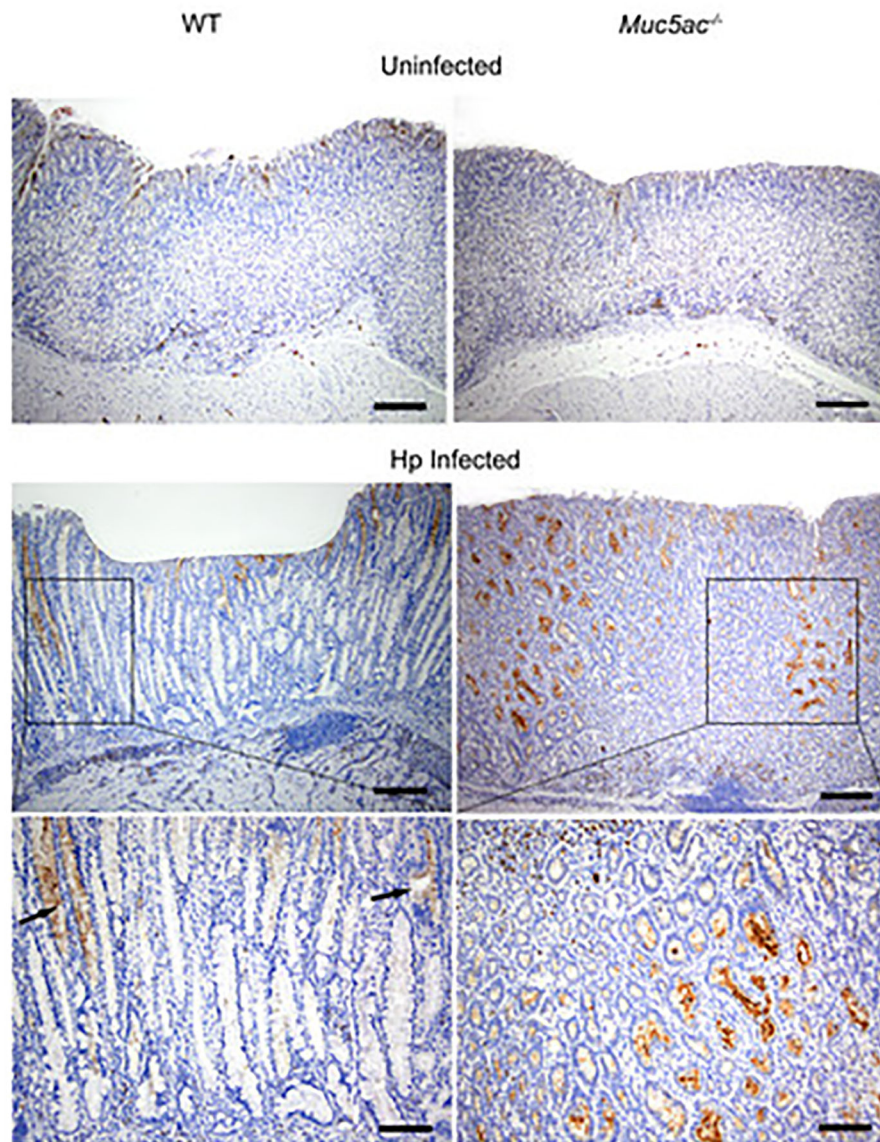
Figure 7: Immunohistochemistry of Clusterin in stomach

In both the uninfected WT and *Muc5ac*$^{-/-}$ gastric corpus epithelium, clusterin is rarely detected except patchy staining of a few foveolar cells at 32 wpi. In *Hp*-infected animals, Clusterin staining is enhanced in a significant proportion of the glands showing pseudopyloric metaplasia (*Muc5ac*$^{-/-}$, low and high magnification, middle and bottom right images respectively) and mostly absent in areas of severe mucous metaplasia (WT stomach, middle and bottom left images). A subset of glands undergoing mucous metaplasia also express the SPEM marker, Clusterin (arrows, left bottom image), Bars: Top 4 images- 160µM, Bottom 2 images- 80µM
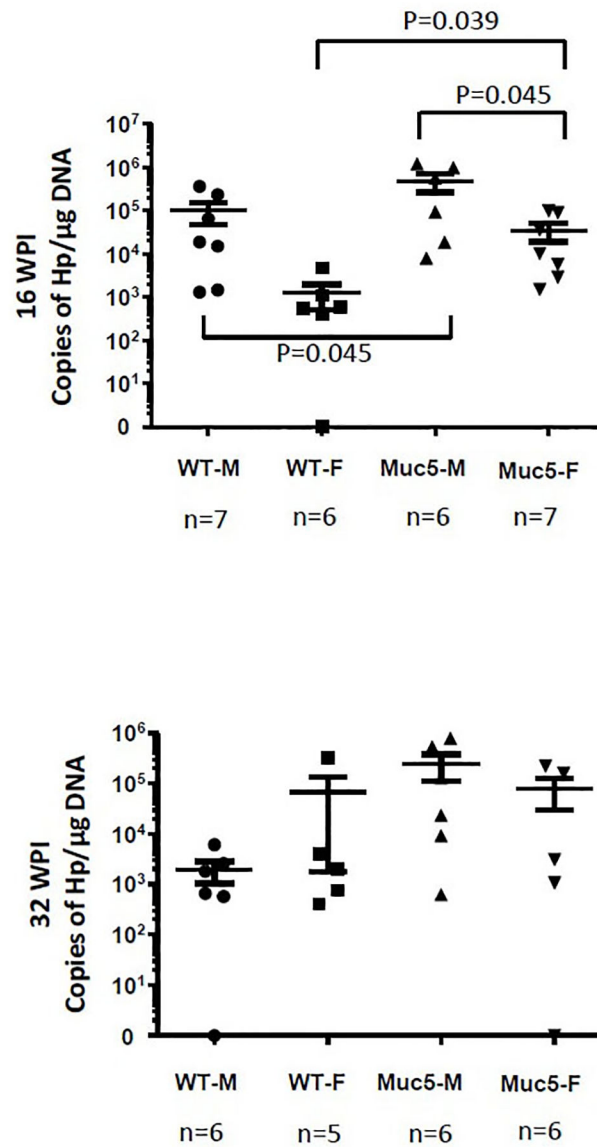
Figure 8: Gastric *Hp* colonization levels

Bacteria abundance was determined in gastric tissues by qPCR using a specific primer set for *Hp* DNA at 16 and 32 weeks post-infection (wpi). Selected p values are displayed in the panels. WT- wild type, M- male, F- Female, Muc5- *Muc5ac^−/−* mice, *Hp*- *Hp* SS1 infection, C- uninfected controls.

Author Manuscript

Author Manuscript
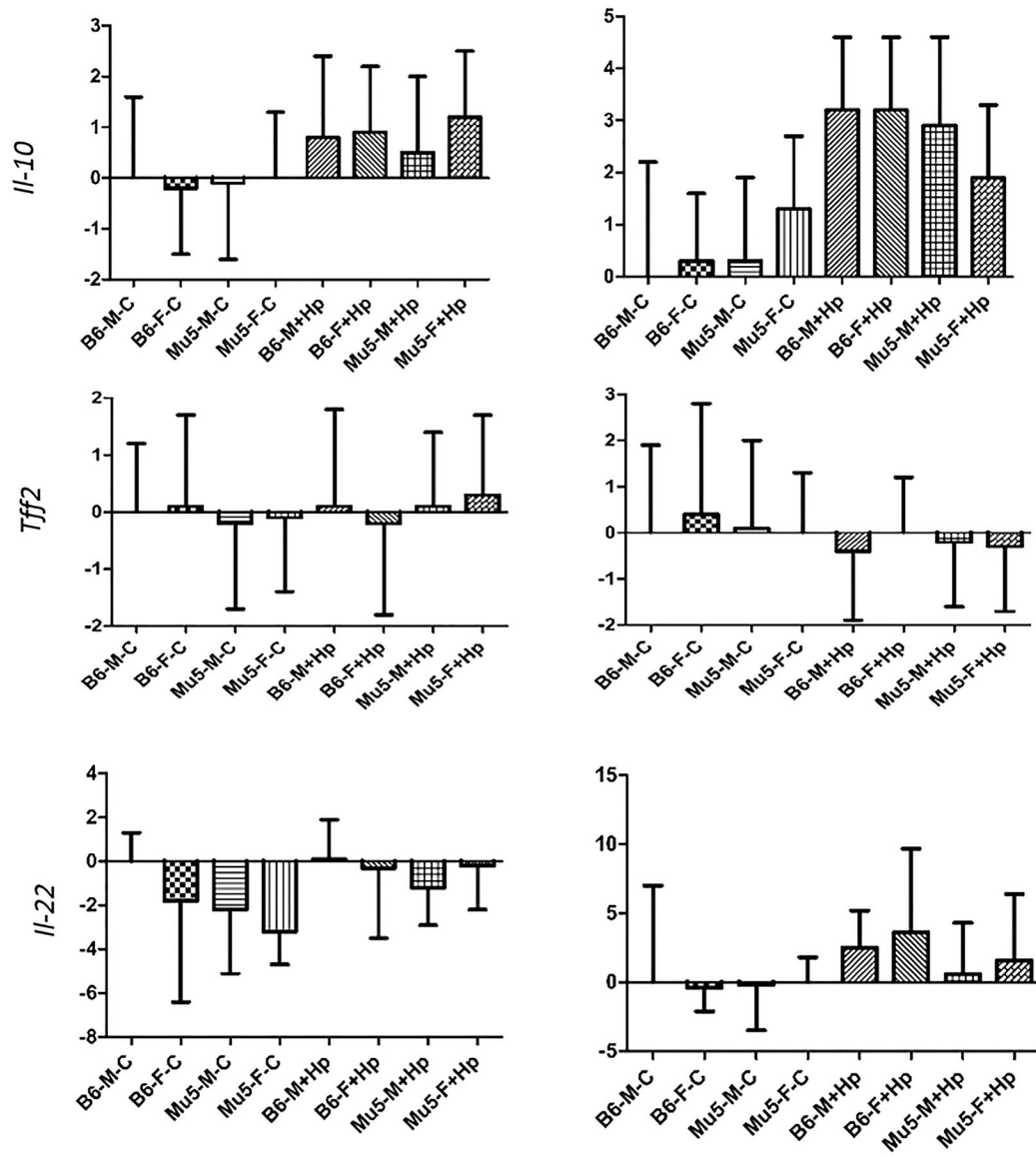
Author Manuscript

Author Manuscript
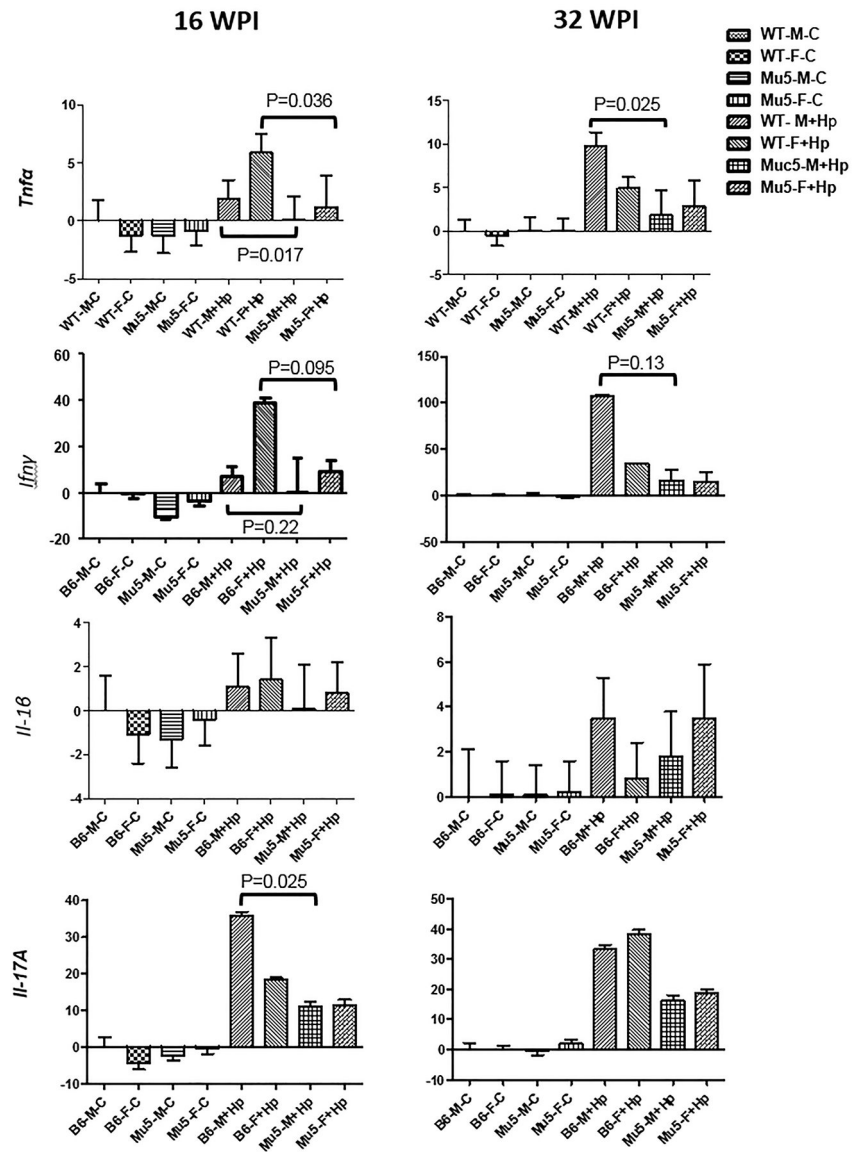
Figure 9 (Panels 1 and 2): mRNA expression levels of inflammatory murine cytokines in the gastric corpus.

Differential expression of inflammatory cytokines was determined in gastric tissues by qPCR using gene specific primer sets at 16 and 32 wpi. Selected p values are displayed in the panels. WT- wild type, M- male, F- Female, Muc5- Muc5ac−/− mice, *Hp*- *Hp* SS1 infection, C- uninfected controls

Table 1:

Animals and Experimental groups:

Mice[*]	Dosing	Timepoint	Sex	#
WT	Sham	16 wpi	M	6
			F	4
		32 wpi	M	5
			F	5
Muc5ac−/−	Sham	16 wpi	M	5
			F	6
		32 wpi	M	6
			F	6
WT	H. pylori	16 wpi	M	7
			F	7
		32 wpi	M	6
			F	5
Muc5ac−/−	H. pylori	16 wpi	M	6
			F	7
		32 wpi	M	7
			F	6

[*]
All mice are on a C57Bl/6–129 0la background as described earlier in the methods

Table 2:

Distribution of various dysplastic lesions in the stomach of *Muc5ac*$^{-/-}$ and WT mice

Gastric antrum/pylorus		No of mice per group and lesion category/(%Incidence)					
		MIT mice 10 months/32wpi				NIEHS mice 10 months/32wpi	
		WT Uninfected (n=10)	WT Hp (n=11)	*Muc5ac*$^{-/-}$ Uninfected (n=12)	*Muc5ac*$^{-/-}$ Hp (n=13)	WT Uninfected (n=11)	*Muc5ac*$^{-/-}$ Uninfected (n=11)
Lesion category	Dysplasia/ Neoplasia score						
Normal epithelium	0	6 (60%)	4 (37%)	1 (10%)	3 (23%)	10 (90%)	1 (9%)
Simple epithelial hyperplasia	0	3 (30%)	5 (45%)	2 (17%)	5 (38%)	0	2 (18%)
Reactive epithelium (indefinite for dysplasia)	1	1 (10%)	2 (18%)	2 (17%)	1 (8%)	1 (10%)	2 (18%)
Atypical hyperplasia (indefinite for dysplasia)	2	0	0	5 (42%)	3 (23%)	0	4 (22%)
Low grade dysplasia/ intraepithelial neoplasia or low grade adenoma	2.5	0	0	**1 (8%)**	**1 (8%)**	0	**1 (9%)**
High grade dysplasia/ intraepithelial neoplasia or a high grade adenoma	3	0	0	**1 (8%)**	0	0	**1 (9%)**
Intramucosal invasive neoplasia (intramucosal carcinoma)	3.5	0	0	0	0	0	0